Defect Structure and Properties of Sr-Doped La Cr O$_{3-\delta}$

Mahmoud OMARI[1*]**, Ilhem CHADLI**[1]**, Salah BELAIDI**[2]
[1]*Département de Chimie, Université de Biskra, B.P. 145,*
07000 Biskra-ALGERIA
e-mail: mahmoud.omari@caramail.com
[2]*Département de Chimie, Université d'Ouargla, B.P. 511,*
30000 Ouargla-ALGERIA

A defect chemical model for the behavior of acceptor-doped LaCrO$_3$ as a function of oxygen pressure is proposed. This is considered within the regime that corresponds to oxygen deficit oxygen. The mathematical approach allows us to calculate the oxygen partial pressure dependant properties of La$_{1-x}$Sr$_x$Cr O$_{3-\delta}$ in the range $0.10 \leq x \leq 0.30$. The results show that the conductivity was independent of pO$_2$ and was proportional to the dopant concentration at high pO$_2$. Therefore, under reducing conditions, the conductivity decreased exponentially with decreasing pO$_2$ and asymptotically approached a pO$_2^{1/4}$ relationship.

Stability regimes and compensation mechanisms at various oxygen partial pressures and temperatures are proposed. This model also examines the charge compensation mechanisms that dominate under the different regimes and their implications for transport properties. From equilibrium constants, thermodynamic quantities such as standard enthalpy and entropy change for the defect formation reactions were calculated.

Key Words: Defect modeling, LSC, Perovskite, Nonstoichiometry, Conductivity.

Introduction

Solid oxide fuel cells (SOFCs) are environmentally clean and highly efficient devices used to generate electricity electrochemically. Limited by the oxygen conductivity of the electrolyte, the most widely studied zirconia-based SOFCs must operate at about 1000 °C. Such high operating temperatures cause electrode reaction and other engineering difficulties. Many efforts are still underway to find alternative electrolytes with higher conductivity at lower temperatures. Among these are studies that have been carried out on bismuth–based mixed oxides such Bi$_2$O$_3$- Ln$_2$O$_3$(Ln = La, Nd, Sm, Dy, Er, Yb)[1] and Bi$_2$O$_3$-Sm$_2$O$_3$-V$_2$O$_5$-MO (M = Pb, Ni, Co) [2].

---

*Corresponding author

The perovskite-type oxide solid solutions La_{1-x} Sr_x M $O_{3-\delta}$(M = Cr, Mn, Fe, Co,)[3-5] and recently $La_{1-x}Ae_x$ M $O_{3-\delta}^6$ have been extensively studied due to their potential application as an air electrode in high-temperature oxide fuel cells, chemical sensor elements and electrodes for magnetohydrodynamic (MHD) generators, because some of them show high catalytic activity. Several useful properties of these perovskite-type oxides such as electrical conductivity and electron emission are the result of their nonstoichiometry and electronic structure. Partial replacement of lanthanum by strontium leads to increased electronic disorder and to changes in the oxidation state of the 3d transition metal and in the oxygen nonstoichiometry. The properties of the perovskite-type oxide are generally quite sensitive to oxygen deficiency and A-site composition. In spite of the importance of oxygen nonstoichiometry, limited studies have been performed, so far, on the nonstoichiometry and the related defect structure of $La_{1-x}Sr_x$ Cr O_3. Mizusaki et al. measured the nonstoichiometry δ for the La_{1-x} Sr_xCrO_3 (x = 0.1-0.3) as a function of temperature, T, and oxygen partial pressure, pO_2[7]. Faber et al. suggested that the conductivity of $La_{0.84}Sr_{0.16}$ Cr O_3 arises from the presence of multivalent Cr ions due to Sr doping[8]. For these purposes, the conduction behavior under low oxygen pressures must be investigated, since if an appreciable electronic conduction arises as a result of defect equilibrium at low pO_2 its electrical conduction is determined by the concentration of present defects in the system. Several years ago, Spinolo et al. suggested a general mathematical method to calculate defect concentrations but without application to actual oxides[9,10]. Recently, Poulsen proposed a defect model for calculating defect concentrations in proton containing perovskites[11] and LSM[3] within a wide range of partial pressure of oxygen.

The purpose of the present work is to establish a defect model equilibrium of La_{1-x} Sr_xCr $O_{3-\delta}$ for the range $0.10 \leq x \leq 0.30$ using the nonstoichiometry data that were reported by Mizusaki et al. [7]. The present defect model will allows us to interpret the thermogravimetric results in which oxygen vacancies are assumed for the oxygen deficient condition. The relationship between the obtained results and those of conductivity measurements[8,12] will also be discussed. Finally, from equilibrium constants, thermodynamic quantities such as standard enthalpy and entropy change for the defect formation reactions are calculated.

Defect Chemical Model

The defect model proposed here is considered within the regime that corresponds to oxygen deficit oxygen. Only 1 sublattice of La_{1-x} $Sr_x Cr$ $O_{3-\delta}$ is assumed to be defected. Reduction of this system leads to an oxygen deficit in the oxygen sublattice. Interactions between defects and interstitial oxygen are neglected. This model is a random point defect model, based on the presence of 2 oxidation states of chromium Cr (Cr^{4+}) and Cr· (Cr^{4+}) that are populated in various proportions depending on temperature, partial pressure of oxygen and Sr -doping. It does not take into account activity coefficients of all present species. The oxygen nonstoichiometry δ assumes negative values, which is explained by the presence of oxide ion vacancies. In the point defect model, the oxygen vacancies are assumed to be fully ionized at high temperatures. In common with earlier work[13-16], this treatment ignores the Schottky defect equilibrium for which, in any case, the equilibrium constant is not available.

For the treatment of point defects in this system we chose the "Kröger-Vink notation"[17]. We therefore define vacancies as particles that occupy a defined site in a crystal and that may have a charge. Sites in a crystal are the points where the atoms or the vacancies may be. For a crystal composed of 2 kinds of atoms we have, for example, the "cationic-sites" and the "oxygen-sites". A point, a negative charge, marks the

positive excess charge by a dash to distinguish this relative charge from the absolute charge.

Adopting this type of notation we obtain on the whole a set of independent equations containing the 3 concentrations of the different species (Table 1), these are

Table 1. Different species used in this defect model with Kröger-Vink notation.

Cationic site	Anionic site
Cr $^{\cdot}$ (Cr^{4+})	O$_O^x$
Cr^x (Cr^{3+})	VÖ
Sr ' (Sr^{2+})	

- The charge-neutrality condition leads to

$$2(V\ddot{o}) + (Cr^{\cdot}) = (Sr') \tag{1}$$

- The value of (Sr ') is given by the nominal A-site composition x. That is

$$(Sr') = x \tag{2}$$

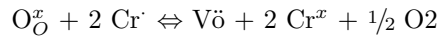Because this solid solution is an oxygen deficient type, we have

$$(V\ddot{o}) = \delta \tag{3}$$

From equations (1)-(3), we have: x = 2 δ + (Cr$^{\cdot}$) $\tag{4}$

With decreasing pO$_2$, (Cr$^{\cdot}$) becomes sufficiently low so that x $\approx$ 2 δ $\tag{5}$

where in Kröger-Vink notation Sr$'$ and Cr$^{\cdot}$ denote, respectively, the Sr^{2+} and Cr^{4+} cations on a Cr^{3+} lattice position.

- Reaction redox leading to oxygen vacancies

$$O_O^x + 2\ Cr^{\cdot} \Leftrightarrow V\ddot{o} + 2\ Cr^x + \tfrac{1}{2}\ O2$$

Oxygen vacancies VÖ are formed and Cr^{4+} (Cr$^{\cdot}$) cations are reduced to Cr^{3+} (Cr^x) at low oxygen partial pressures.

$$Kox = (V\ddot{o}).(Cr^x)^2.pO_2^{1/2}/[(O^x).(Cr^{\cdot})^2] \tag{6}$$

In order to maintain the fixed A/ B ratio, the following equation must be maintained:

$$(Cr^{\cdot}) + (Cr^x) = 1 \tag{7}$$

Kröger-Vink notation[17] is used with La (+3) Cr (+3) O$_3$ as the reference state.

The experimental nonstoichiometry data as a function of pO$_2$ are fitted to equation (6) taking the equilibrium constant as a fitting parameter.

(VÖ): test value in the interval 10^{-20} to 0.5. The step-wise calculation proceeds as follows:

We assume a value for (VÖ)

$$(O_O^x) = 3 - (V\ddot{o}) \tag{8}$$

From equation (7) we obtain

$$(Cr^{\cdot}) = 1 - (Cr^x) \qquad (9)$$

By substituting $(Cr^{\cdot})$ in equation (4) one obtains the following expression:

$$(Cr^x) = 1 + 2\delta - x \qquad (10)$$

If the set of concentrations is accepted, we can insert (Vö), (O_O^x), (Cr^x) and $(Cr^{\cdot})$ into equation (6) and find the oxygen partial pressure that corresponds to the equilibrium concentrations. The calculation is next performed for a new value of (Vö) until all the concentration interval of interest has been covered.

Results and Discussion

The simulations are normally made for an interval (Vö) from an arbitrarily chosen lowest limit of 10^{-20} up to 0.5. Solutions are normally generated for a very wide pO$_2$ span from 10^{-25} to 1 atm. Calculation and plotting of all concentrations at different pO$_2$ s are carried out on a Pentium IV. The equilibrium constants used in the following are calculated using nonstoichiometric values TG-data[7].

Defect concentration in $La_{1-x}Sr_xCr\ O_{3-\delta}$

For the comparison, we chose to present for all species and in the same defect diagram their concentrations as a function of pO$_2$. Figure 1 shows the defect diagram for LSC10 with all kinds of vacancies and metal. It can be easily seen from the plot that for pO$_2 > 10^{-18}$ atm the predominant ions are Cr^{3+}. There are no physical solutions for the set of 3 concentrations at pO$_2 < 10^{-18}$ atm where $(Cr^{\cdot})$ concentration goes negative, i.e. all chromium is in oxidation state +3, at O total / Cr $\approx$ 2.5.
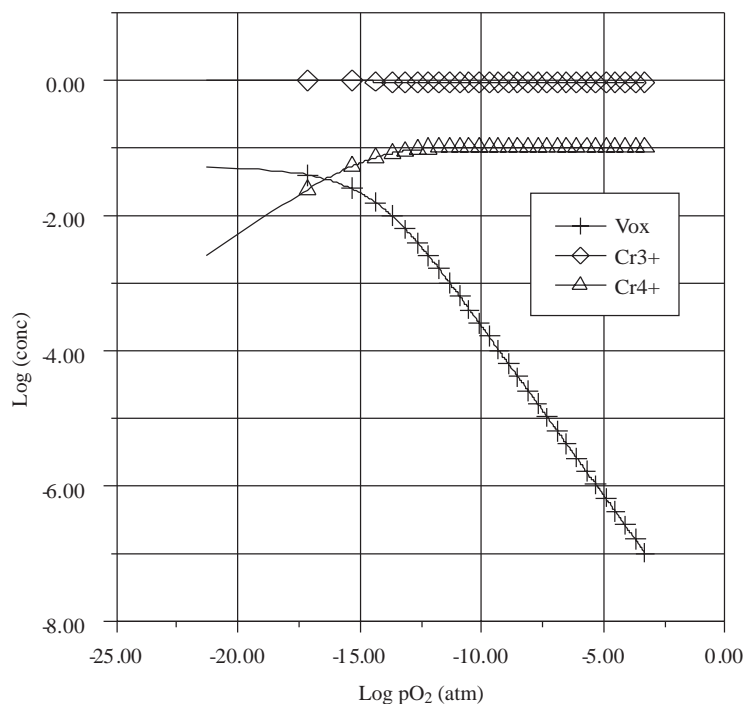
Figure 1. Defect diagram for LSC10 at 1000 °C.

The relative carrier concentration for LSC10 as a function of pressure at different temperatures is shown in Figure 2. The variation of $(Cr^{\cdot})$ for $La_{0.75}$ $Sr_{0.25}Cr$ O_3 as a function of partial pressure calculated by Van Hassel et al. [18] is similar to the obtained results (Figure 1) for LSC10. In the ionic compensation charge, the carrier concentration appears to be in agreement with pO_2 dependence proposed by the model within the temperature range investigated (1000 to 1300 °C). As expected, the figure further indicates that, in the intermediate pO_2 range, where electronic compensation predominates, the carrier concentration is independent of both temperature and pO_2. The transition from pO_2 dependence to independence shifts to higher oxygen partial pressure as the temperature of equilibration increases from 1000 to 1300 °C. A plot of log carrier concentration as a function of $pO_2^{1/4}$ is expected to be linear in the region where ionic compensation is predominant. Critical pO_2 corresponding to the reduction and the oxidation of chromium shifted to higher pO_2 when the temperature increased. At $pO_2 > 10^{-12}$ atm, log (Cr^{4+}) is practically constant and equal to -1. The concentration dependence with pO_2 at low and high values of partial pressure is similar to that of LSM^3.
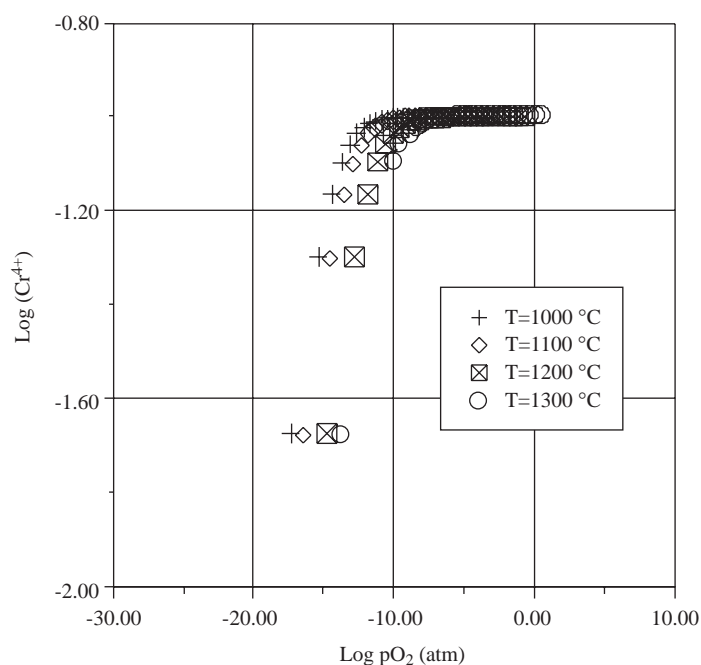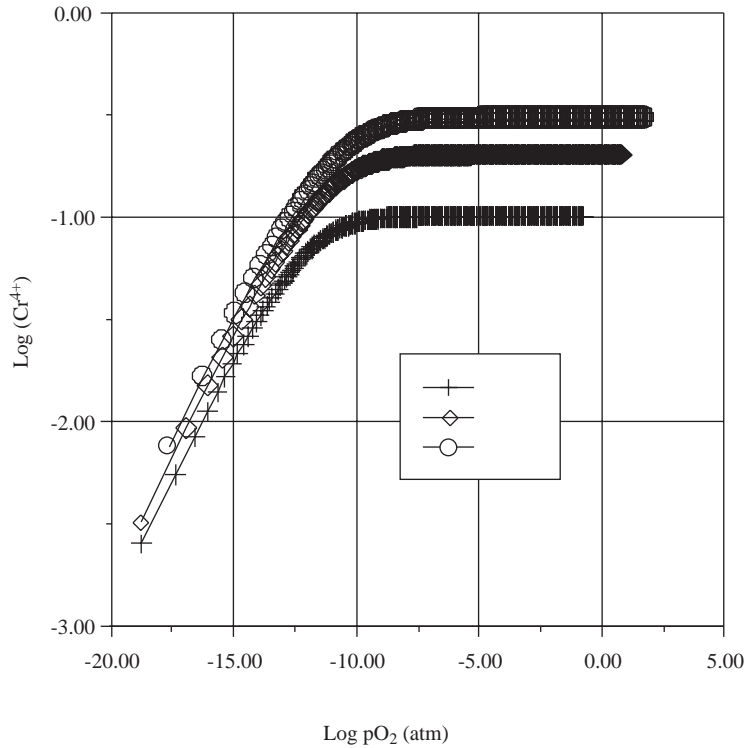

Figure 2. Relative carrier concentration as a function of pO_2 and temperature for LSC10.

The effect of Sr content at 1200 °C on the carrier concentration is shown in Figure 3. The relative carrier concentration appears to have a one-fourth power dependence on pO_2 in the region where oxygen compensation is expected ($pO_2 < 10^{-8}$ atm). The Figure also indicates that the transition from ionic to electronic compensation occurs at relatively higher pO_2 as the Sr content increases, as expected from the model.

The calculated nonstoichiometry as a function of pO_2 for LSC10, LSC20 and LSC30 at 1200 °C is presented in Figure 4. At constant temperature, the critical pO_2 is higher for the composition with higher strontium content. At lower pO_2 the amount of oxygen nonstoichiometry reaches the limit $\delta = (x/2)$ as predicted from equation (4). This plateau corresponds to a new stoichiometric state where all chromium is in Cr^{3+}. Oxygen vacancy begins to form at 10^{-10} to 10^{-8} atm of pO_2. The calculated nonstoichiometry

isotherms are in good agreement with the reported thermogravimetry data[3] and similar to those obtained for Ca- doped LaCrO$_3^{19}$. These results conform very well to those obtained for the dependence of carrier concentration with pO$_2$ (Figure 3).


Figure 3. Relative carrier concentration as a function of pO$_2$ and composition at 1200 °C for LSC10.
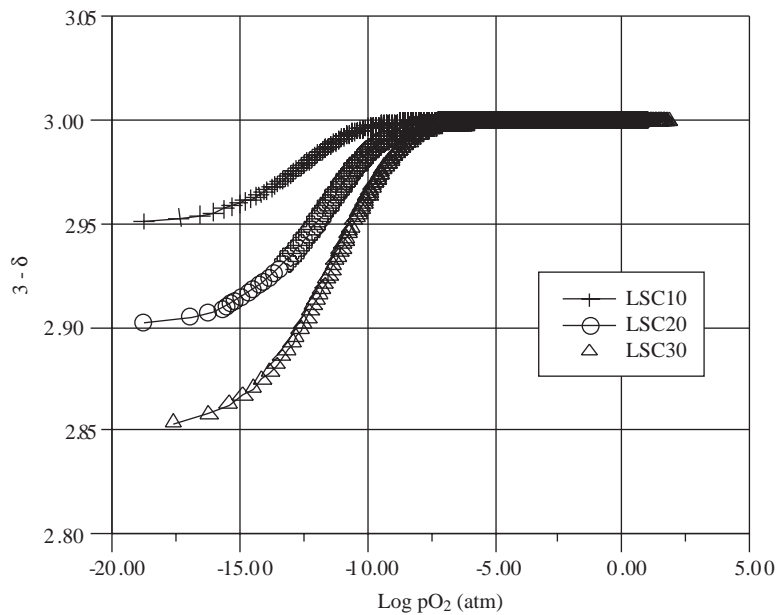
Figure 4. Simulated oxygen nonstoichiometry at 1200 °C for 3 different compositions, LSC10, LSC20 and LSC30.
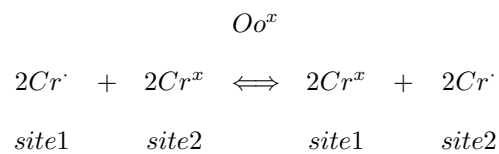
The effect of temperature on oxygen nonstoichiometry of LSC10 is shown in Figure 5. At higher temperatures, oxygen vacancies begin to form at higher pO_2 (10^{-11} to 10^{-8} atm) and their amounts approach the constant values at lower pO_2 ($\sim 10^{-20}$ atm), which corresponds to a new stoichiometric state. In this case also, we see a good agreement between these results and those concerning the effect of temperature on the relative carrier concentration (Figure 2). This behavior is the same as that was found in Ca- doped $LaCrO_3^{19}$. The critical pO_2 range corresponding at the transition from the ionic to the electronic compensation charge is practically the same (10^{-11} to 10^{-8} atm).
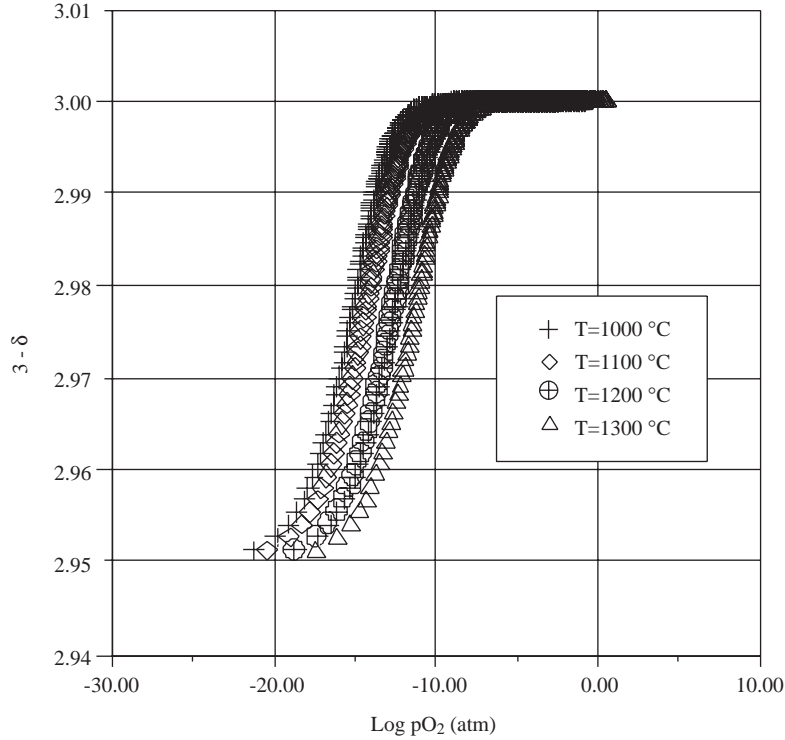
Figure 5. Simulated oxygen nonstoichiometry of LSC10 as a function of oxygen partial pressure at 4 different temperatures.

Electrical Conductivity

Total conductivity is the summation of the individual contributions from ionic and electronic carriers. Each term is a product of the numerical value of the charge of the carrier, the relative concentration of the carrier and the kind of mobility for that carrier. The electron transport can be formulated as a charge transfer reaction as follows:

$$Oo^x$$

$$2Cr^{\cdot} \quad + \quad 2Cr^x \quad \Longleftrightarrow \quad 2Cr^x \quad + \quad 2Cr^{\cdot}$$

$$site1 \qquad site2 \qquad\qquad site1 \qquad site2$$

$$\sigma_{total} = \sigma_e + \sigma_{ion} \tag{11}$$

Poulsen[7] has proposed an expression of total conductivity as a function of different concentration species.

$$\sigma_{total} = m_e.(Cr^\cdot).(Cr^x) + m_{ion}.|-2|.(O_O^x).(V\ddot{o}) \qquad (12)$$

where m$_e$ and m$_{ion}$ represent electronic and ionic mobility respectively.

Figure 6 presents the dependence of conductivities on oxygen partial pressure as a function of composition at 1200 °C. All compositions showed common characteristics:

Little pO$_2$ dependence was observed in a range of high pO$_2$ and this range narrows with increasing temperature.

As reduction proceeded, the electrical conductivity decreased with approximately pO$_2^{1/4}$.

An abrupt decrease in electrical conductivity occurred under high reducing conditions.

The critical pO$_2$ shifted to higher pO$_2$ when the temperature and / or the dopant concentration were increased.
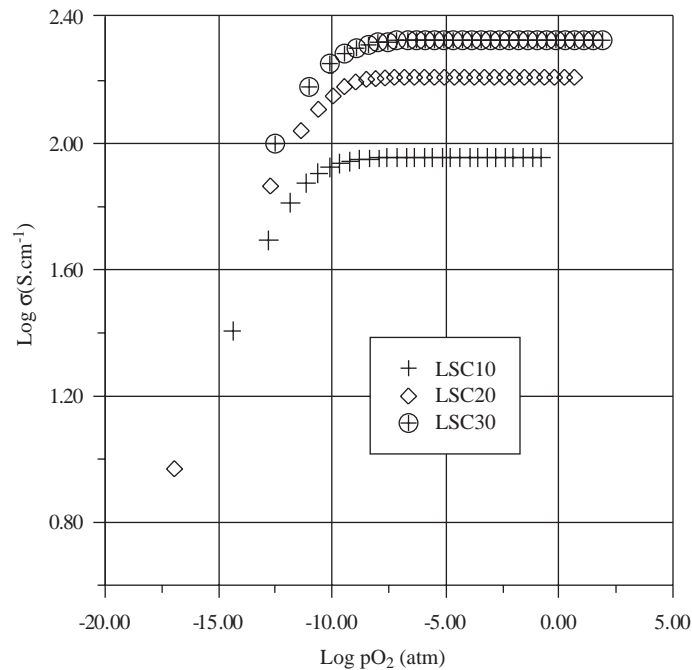

Figure 6. Conductivity isotherms at 1200 °C for three different compositions LSC10, LSC20 and LSC30

The electrical conductivity appears to have a one-fourth power dependence on the oxygen partial pressure in the region (10^{-20} to 10^{-8} atm). The figures also indicate that the transition from ionic to electronic compensation occurs at relatively higher pO$_2$ as the Sr content increases, as expected from the model.

The effect of temperature on the conductivity for LSC10 is shown in Figure 7. In the ionic compensation region, the electrical conductivity dependence on oxygen partial pressure proposed by this model is in good agreement with Meadowcroft's work[12]. This behavior is similar to that observed in Ca-doped LaCrO$_3$[19,20] and LSM[3]. As expected, the figure further indicates that, in the intermediate pO$_2$ range, where electronic compensation predominates, the conductivity is independent of both temperature and pO$_2$. The transition from pO$_2$ dependence to independence shifts to higher oxygen partial pressure as the temperature

of equilibration increases from 1000 to 1300 °C. These results are in close agreement with the reported conductivity measurements[8,12].
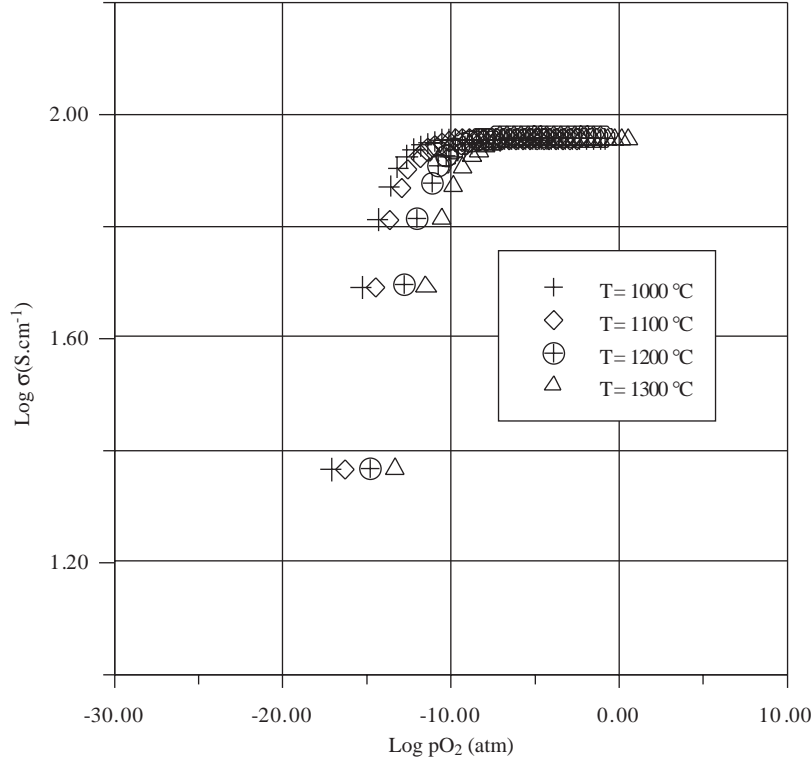
Figure 7. Electrical conductivity of La$_{0.9}$ Sr $_{0.1}$Cr O$_{3-\delta}$ as a function of pO$_2$ at 4 temperatures.

The conductivity at high pO$_2$ has a weak pO$_2$ dependence, the product (Cr$^{\cdot}$). (Cr^{x}) is constant until 10^{-11}atm and the conductivity decreases with an approximate slope ∂ (log σ) / ∂ (log pO$_2$) $\approx$ 0.14. This is in accordance with the experiments[8,12]. Faber et al. suggested that La$_{0.84}$ Sr$_{0.16}$ CrO$_3$ is a p-type conductor and its conductivity arises from the presence of multivalent Cr ions due to Sr doping[8]. The constant electrical conductivity that exists in the high pO$_2$ region may be easily understood if it is assumed that acceptors control the carrier concentration and that the electronic compensation predominates. In the lower pO$_2$ region, oxygen vacancies are formed and the electrical conductivity begins to decrease due to ionic charge compensation. The conductivity mechanism in acceptor-doped lanthanum chromites is due, as mentioned in the literature, to small - polaron hopping irrespective of the kinds of dopants[21,22].

Thermodynamic considerations of the defect model

Some useful thermodynamic quantities such as $\Delta G°ox$, the standard free energy change, $\Delta S°ox$ the standard entropy and $\Delta H°ox$ the standard enthalpy change for the reaction of equation (6) can be easily calculated according the following equations:

$$\Delta G°ox = -RT \ln Kox = \Delta H°ox - T\Delta S°ox \qquad (13)$$

$$\Delta S°ox = -\partial(\Delta G°ox)/\partial T \qquad (14)$$

and

$$\Delta H^{\circ}ox = \Delta G^{\circ}ox + T\Delta S^{\circ}ox \tag{15}$$

These quantities are calculated for LSC10 and LSC30 using the equilibrium constants (Table 2) by the least-squares method and are shown in Tables 3 and 4. The enthalpy of the reaction was obtained from the slope of the Arrhenius plot. The $\Delta S^{\circ}ox$ values depend on the composition x and are relatively close to those obtained for La$_{1-x}$ Sr$_x$ Fe O$_3^{23}$. The slight difference from values of $\Delta H^{\circ}ox$ and $\Delta S^{\circ}ox$ for the same Sr- doped LaCrO$_3^7$is due to interactions between defects that we do not take into account in the present defect model. The changes in standard enthalpy and standard entropy show a composition dependence with acceptor-dopant. These were estimated to be -74.97 Kcal/mol and -23.36 cal.mol^{-1}.K^{-1} for La$_{0.9}$ Sr$_{0.1}$Cr O$_{3-\delta}$, -80.21 Kcal/mol and -28.04 cal.mol^{-1}.K^{-1} for La$_{0.9}$ Sr$_{0.3}$Cr O$_{3-\delta}$ respectively. From these results, the standard enthalpy depends strongly on composition, so the ideal solution approximation cannot be applied to the Sr concentration change. This behavior was also suggested for La$_{1-x}$ Sr$_x$Cr O$_{3-\delta}$ and La$_{1-x}$ Sr$_x$Co O$_{3-\delta}$ by Mizusaki[4], which is in good agreement with the nonstoichiometry data[24,25].

Table 2. Equilibrium constants for LSC10 and LSC30.

Temperature (°C)	Kox (x = 0.1)	Kox (x = 0.3)
1000	6 10^{-8}	3.7 10^{-8}
1100	1.57 10^{-7}	1.89 10^{-7}
1200	1.12 10^{-6}	1.32 10^{-6}
1300	5.08 10^{-6}	1.46 10^{-5}

Table 3. Standard enthalpy and entropy change for the formation of oxygen vacancies.

Compound	$\Delta H^{\circ}ox$ (Kcal/mol)	$\Delta S^{\circ}ox$ (cal.mol^{-1} .K^{-1})
La$_{0.9}$ Sr$_{0.1}$Cr O$_{3-\delta}$	-74. 97	-23.36
La$_{0.7}$ Sr$_{0.3}$Cr O$_{3-\delta}$	-80.21	-28.04

Table 4. Standard free energy change for the formation of oxygen vacancies for LSC10.

Temperature (°C)	$\Delta G^{\circ}ox$ (Kcal/mol)
1000	-42.34
1100	-43.02
1200	-40.29
1300	-38.35

Conclusion

The data obtained from TG experiments support the proposed defect model for the oxidation behavior of acceptor-doped LaCrO$_3$. This defect model indicates that at high pO$_2$ electronic compensation occurs by a transition of Cr^{3+} to Cr^{4+}, whereas ionic compensation takes place at lower pO$_2$ by the formation of oxygen vacancies. The oxygen partial pressure at which electronic compensation shifts to ionic is both acceptor-dopant and temperature dependent. The general behavior is that the transition shifts to higher oxygen partial pressure as the temperature or the concentration of acceptor-dopant increases. The phase stability of Sr-doped LaCrO$_3$ against reduction was shifted to higher pO$_2$ when the temperature and / or Sr-dopant

concentrations increased. The changes in standard enthalpy and standard entropy show a composition dependence with acceptor-dopant. They were estimated to be -74.97 Kcal/mol, -23.36 cal.mol^{-1}.K^{-1} for La$_{0.9}$ Sr$_{0.1}$Cr O$_{3-\delta}$ and -80.21 Kcal/mol,-28.04 cal.mol^{-1} .K^{-1} for La$_{0.9}$ Sr $_{0.3}$Cr O$_{3-\delta}$ respectively.

Acknowledgments

References

1. H. Iwahara, T. Esaka and T. Sato, **J. Solid State Chem.**, **39**, 173 (1981).

2. M. Benkaddour, M. Omari, J.C. Boivin, P. Conflant and M. Drache, **Ann. Chim. Sci. Mat**. **25 (S1)**, 165 (2000).

3. F.W. Poulsen, **Solid State Ionics**, **129**, 145 (2000).

4. J. Mizusaki, M. Yoshihiro,S. Yamauchi and K. Fueki , **J. Solid State Chem.**, **67**, 1 (1987).

5. M.H.R. Lankhorst, H.J.M. Bouwmeester and H. Verweij, **Solid State Ionics**, **96**, 21 (1997).

6. E. Bakken, T. Norby and S. Stolen, **J. Mat. Chem.**, **12**, 317 (2002).

7. J. Mizusaki, S. Yamauchi, K. Fueki and A. Ishikawa, **J. Solid State Chem.**, **12**,119 (1984).

8. J. Faber, M. Mueller, W. Procarione, A. Aldred and H. Knott, **Conference on High Temperature Science Related to Open Cycle**, **Cool Fired MHD Systems**. Argonne National Laboratory, Argonne, IL, April 1977.

9. G. Spinolo and U. Anselmi-Tamburini, **Ber. Bunsenges. Phys. Chem**, **99** , 87 (1995).

10. G. Spinolo, U. Anselmi-Tamburini and P. Ghigna, **Z. Für Naturforschung**, **A52**, 629 (1997).

11. F.W. Poulsen, **J. Solid State Chem.**, **143** , 115 (1999).

12. D.B. Meadowcroft, **Br. J. Appl. Phys.**, **9**, 1225 (1969).

13. H. Uchida, H. Yoshikawa and H. Iwahara, **Solid State Ionics**, **35**, 229 (1989).

14. Y. Larring and T. Norby, **Solid State Ionics**, **97**, 523 (1997).

15. T. Schober and H. Wenzl, **Ionics**, **81**, 111 (1995).

16. T. Schober, W. Schilling and H. Wenzl, **Solid State Ionics**, **86-88**, 653 (1996).

17. F.A. Kröger and H.J. Vink, **Solid State Physics**, Vol. 3, p. 307, eds. by F. Seitz and D. Turnbull. Academic Press, New York, 1956.

18. B.A. Van Hassel, T. Kawada, N. Sakai, H. Yokokawa, M. Dokiya and H.J.M. Bouwmeester **Solid State Ionics**, **66**, 295 (1993).

19. I. Yasuda and T. Hikita, **J. Electrochem. Soc.**, **140**, 1699-1704 (1993).

20. H. Kamata, Y. Yononemura, J. Mizusaki, H. Tagawa, K. Naraya and T. Sasamoto, **J. Phys. Chem. Solids**, **56,** 943-50 (1995).

21. D.P. Karim and A.T. Aldred, **Phys. Rev**. B, **20**, 1255 (1979).

22. J.B. Webb, M. Sayer and A. Mansingh, **Can. J. Phys**., **55**, 1725 (1977).

23. J. Mizusaki, M. Yoshihiro, S. Yamauchi and K. Fueki, **J. Solid State Chem.**, **58**, 257 (1985).

24. M.H.R. Lankhorst, H.J.M. Bouwmeester and H. Verweij, **J. Solid State Chem.**, **133**, 555 (1997).

25. J. Mizusaki, Y. Mima, S. Yamauchi and K. Fueki , **J. Solid State Chem.**, **80**, 102 (1989).